Recommended Practices in Thrust Measurements

IEPC-2013-440

James E. Polk,* Anthony Pancotti,† Thomas Haag,‡ Scott King,§ Mitchell Walker,¶
Joseph Blakely‖, John Ziemer**

Accurate, direct measurement of thrust or impulse is one of the most critical elements of electric thruster characterization, and one of the most difficult measurements to make. The American Institute of Aeronautics and Astronautics has started an initiative to develop standards for many important measurement processes in electric propulsion, including thrust measurements. This paper summarizes recommended practices for the design, calibration, and operation of pendulum thrust stands, which are widely recognized as the best approach for measuring μN- to mN-level thrust and μNs-level impulse bits. The fundamentals of pendulum thrust stand operation are reviewed, along with its implementation in hanging pendulum, inverted pendulum, and torsional balance configurations. Methods of calibration and recommendations for calibration processes are presented. Sources of error are identified and methods for data processing and uncertainty analysis are discussed. This review is intended to be the first step toward a recommended practices document to help the community produce high quality thrust measurements.

I.   Introduction

As part of a larger effort by the American Institute of Aeronautics and Astronautics (AIAA) Electric Propulsion Technical Committee to provide standards for electric thruster measurement and test, we have been developing recommended practices for direct thrust measurements. Measurement of thrust is the most fundamental requirement in thruster performance characterization. Because electric thrusters produce relatively low thrust levels, particularly microthrusters that have enjoyed increased attention in the last two decades, direct thrust measurements can be challenging. Considerable effort and talent has been invested in developing sensitive thrust stands and measurement techniques, and one objective of the AIAA initiative is to capture this knowledge and distill it for the community.

The purpose of this paper is not to specify a particular thrust stand design that must be used to produce credible results, but to recommend best practices for the use of the most common types of pendulum thrust stands based on experience from the community. These recommendations include best practices for the design, calibration and operation of pendulum thrust stands and the analysis of thrust stand data with a particular focus on cataloguing sources of error and estimating the uncertainty in the measurements. The goals are to help users avoid common mistakes, improve the quality of thrust stand measurements with proven approaches to thrust stand use, and provide guidelines for reporting results to make it easier to evaluate the reliability of thrust stand measurements.

*Principal Engineer, Propulsion, Thermal and Materials Engineering Section, Jet Propulsion Laboratory, California Institute of Technology, M/S 125-109, 4800 Oak Grove Drive, Pasadena, CA 91109

†Advanced Propulsion Research Scientist, MSNW, LLC, Redmond WA 98052

‡Aerospace Engineer, Space Propulsion Branch, NASA Glenn Research Center, Cleveland, OH 44135

§Graduate Research Assistant, School of Aerospace Engineering, Georgia Institute of Technology, Atlanta, Georgia, 30332

¶Associate Professor, School of Aerospace Engineering, Georgia Institute of Technology, Atlanta, Georgia, 30332

‖Electric Propulsion Research Scientist, ERC, Inc./AFRL Spacecraft Propulsion Branch, Air Force Research Laboratory, Edwards AFB, CA 93523

**Concept Innovation Methods Chief, JPL Innovation Foundry, Jet Propulsion Laboratory, California Institute of Technology, 4800 Oak Grove Drive, Pasadena, CA 91109

Report Documentation Page		Form Approved OMB No. 0704-0188

1. REPORT DATE **OCT 2013**	2. REPORT TYPE	3. DATES COVERED **00-00-2013 to 00-00-2013**

4. TITLE AND SUBTITLE **Recommended Practices in Thrust Measurements**	5a. CONTRACT NUMBER
	5b. GRANT NUMBER
	5c. PROGRAM ELEMENT NUMBER
6. AUTHOR(S)	5d. PROJECT NUMBER
	5e. TASK NUMBER
	5f. WORK UNIT NUMBER

7. PERFORMING ORGANIZATION NAME(S) AND ADDRESS(ES) **California Institute of Technology,Jet Propulsion Laboratory,4800 Oak Grove Drive,Pasadena,CA,91109**	8. PERFORMING ORGANIZATION REPORT NUMBER

9. SPONSORING/MONITORING AGENCY NAME(S) AND ADDRESS(ES)	10. SPONSOR/MONITOR'S ACRONYM(S)
	11. SPONSOR/MONITOR'S REPORT NUMBER(S)

12. DISTRIBUTION/AVAILABILITY STATEMENT
Approved for public release; distribution unlimited

13. SUPPLEMENTARY NOTES

14. ABSTRACT

15. SUBJECT TERMS

16. SECURITY CLASSIFICATION OF:			17. LIMITATION OF ABSTRACT	18. NUMBER OF PAGES	19a. NAME OF RESPONSIBLE PERSON
a. REPORT **unclassified**	b. ABSTRACT **unclassified**	c. THIS PAGE **unclassified**	**Same as Report (SAR)**	**24**	

This paper provides an overview of the three types of pendulum thrust stands, including the dynamics that underly their operation and key performance metrics. Typical implementations and how they are optimized to meet the performance metrics are then described. Methods for calibration, operation, and data analysis are discussed along with typical sources of error, methods to control them, and the process of estimating measurement uncertainties.

II.   Thrust Stands for Electric Propulsion

A.   Overview

High thrust devices are often tested on load cells, where the force is measured directly. However, because most electric thrusters have low thrust-to-mass ratios, the load cell signal is generally overwhelmed by the weight of the thruster. Instead, the thrust or impulse bit from electric thrusters is typically inferred from the motion of pendulum thrust stands. Three major configurations, hanging pendulums, inverted pendulums, and torsional pendulums, are used to make accurate steady state and impulse thrust measurements. All of these configurations are variations of a spring-mass-damper system. While each of these implementations has its advantages and disadvantages, pendulum thrust stands are widely accepted as the best method to take direct thrust measurements with electric thrusters.

B.   Pendulum Thrust Stand Dynamics.

Many characteristics of pendulum thrust stands can be understood by examining two solutions to the equation of motion for ideal pendulums. The equation of motion for a second order system relates the time rate of change of angular momentum to the sum of torques due to torsional springs, dampers, and applied forces.[1] The dynamics of all three types of pendulums are described by the same equation,

$$I\ddot{\theta} + c\dot{\theta} + k\theta = F(t)L, \tag{1}$$

where θ is the angular position relative to a reference position, I is the moment of inertia, c is the damping constant, k is the effective spring constant associated with restoring forces, and $F(t)$ is an applied force acting at a distance L from the pivot which produces a torque on the system. I, c, and k are assumed to be constants. Actual thrust stands may include active components such as electronic dampers where the damping constant is frequency dependent, which complicates the analysis. This equation can be cast in the standard form

$$\ddot{\theta} + 2\zeta\omega_n\dot{\theta} + \omega_n^2\theta = F(t)L/I, \tag{2}$$

where ζ is the damping coefficient,

$$\zeta = \frac{c}{2}\sqrt{\frac{1}{Ik}} \tag{3}$$

and ω_n is the natural frequency of the undamped system,

$$\omega_n = \sqrt{\frac{k}{I}}. \tag{4}$$

The primary difference in the three types of pendulum thrust stands is the effect of the gravity force on the dynamics. Gravity acts as a restoring force in hanging pendulums, a force tending to increase the deflection in inverted pendulums, and has no influence on ideal torsional pendulums where the plane of motion is perpendicular to the gravity vector. The torque associated with the gravitational force in hanging and inverted pendulums is

$$\mathcal{T}_g = mgL_{cm}\sin\theta \simeq mgL_{cm}\theta, \tag{5}$$

where m is the mass, g is the acceleration due to gravity, and L_{cm} is the distance from the center of mass to the pivot point. The second expression is valid for small deflection angles. For example, the error associated with this approximation is less than 0.13% for angles of 5° or less. In this approximation where the gravity

torque is proportional to the deflection, it can be incorporated in the spring torque term of Eqn. (1),

$$k = \begin{cases} k_s + mgL_{cm} & \text{for hanging pendulums} \\ k_s - mgL_{cm} & \text{for inverted pendulums} \end{cases} \tag{6}$$

Clearly, for inverted pendulums the gravity torque must not exceed the spring torque, otherwise the restoring force is negative and the pendulum is unstable.

Equation (2) can be solved to give the response of a pendulum to an arbitrary input force. Three special cases with analytical solutions are particularly relevant for pendulum thrust stands. The dynamic motion of a pendulum thrust stand subject to the torque produced by a constant thrust F_t from a steady state thruster applied at a distance L_t from the pivot can be approximated by the response of an ideal pendulum to a step input, where

$$F(t) = \begin{cases} 0 & \text{for } t < 0 \\ F_t & \text{for } t \geq 0 \end{cases} \tag{7}$$

The deflection $\theta(t)$ normalized by the steady state deflection

$$\theta_{ss} = \frac{F_t L_t}{I \omega_n^2} = \frac{F_t L_t}{k} \tag{8}$$

depends on the damping coefficient,

$$\frac{\theta(t) I \omega_n^2}{F_t L_t} = \frac{\theta(t)}{\theta_{SS}} = \begin{cases} 1 - e^{-\zeta \omega_n t} \left[\cos(\omega_d t) + \frac{\zeta}{\sqrt{1-\zeta^2}} \sin(\omega_d t) \right] & \text{for } \zeta < 1 \text{ (underdamped)} \\ \\ 1 - e^{-\omega_n t}(1 - \omega_n t) & \text{for } \zeta = 1 \text{ (critically damped)} \\ \\ 1 + \frac{1}{2\sqrt{\zeta^2-1}} \left[\frac{1}{d_1} e^{-d_1 \omega_n t} - \frac{1}{d_2} e^{-d_2 \omega_n t} \right] & \text{for } \zeta > 1 \text{ (overdamped)}. \end{cases} \tag{9}$$

In these expressions $\omega_d = \omega_n \sqrt{1 - \zeta^2}$ is the frequency of the damped motion, $d_1 = \zeta - \sqrt{\zeta^2 - 1}$, and $d_2 = \zeta + \sqrt{\zeta^2 - 1}$. Example responses plotted in Fig. (1) show that the time required to reach the steady state deflection depends on the damping coefficient. The settling time, defined as the time required to settle within 2% of the steady state deflection is about one period for critically damped pendulums, and depends on the damping coefficient for overdamped and underdamped pendulums. This is a fundamental limit on the response time for step changes in thrust levels for pendulum thrust stands.
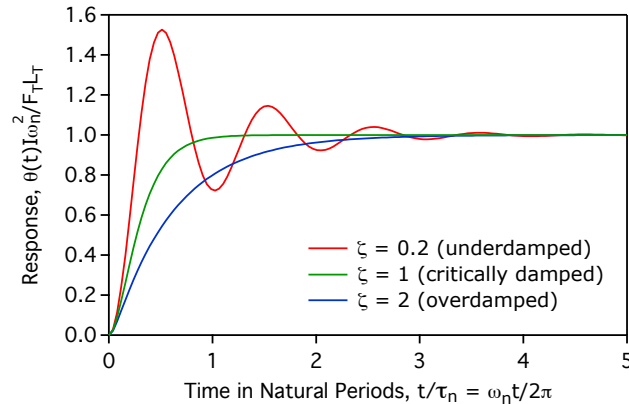

Figure 1. Response of under-, over-, and critically-damped pendulums to a step input, normalized by the steady state deflection.

The response of a pendulum thrust stand to the impulse bit from a pulsed thruster applied at a distance L_t

from the pivot may be approximated by the solution to Eqn. (2) for an impulse input $F(t) = I_{bit}\delta(t)$:

$$\frac{\theta(t)I\omega_n}{I_{bit}L_t} = \begin{cases} \frac{1}{\sqrt{1-\zeta^2}}e^{-\zeta\omega_n t}\sin(\omega_d t) & \text{if } \zeta < 1 \text{ (underdamped)} \\ \\ \omega_n t e^{-\omega_n t} & \text{if } \zeta = 1 \text{ (critically damped)} \\ \\ \frac{1}{2\sqrt{\zeta^2-1}}\left[e^{-d_1\omega_n t} - e^{-d_2\omega_n t}\right] & \text{if } \zeta > 1 \text{ (overdamped)} \end{cases} \quad (10)$$

Example solutions plotted in Fig. (2) show that the response is a transient with a decay time determined by the damping coefficient. As the expanded plot in the upper right portion of this figure suggests, all three curves have the same initial slope, reflecting that fact that the initial angular velocity produced by the impulse is independent of the damping coefficient. This initial velocity is

$$\dot{\theta}(0) = I_{bit}L_t/I \quad (11)$$

It can be also be shown that the maximum amplitude θ_m and the range (difference between the first peak and the first valley) of the response is proportional to the impulse bit. For example, for an undamped oscillator ($\zeta = 0$), the maximum amplitude is

$$\theta_m = I_{bit}L_t/I\omega_n. \quad (12)$$

The peak amplitude and range decrease as the damping coefficient increases. The equations of motion can
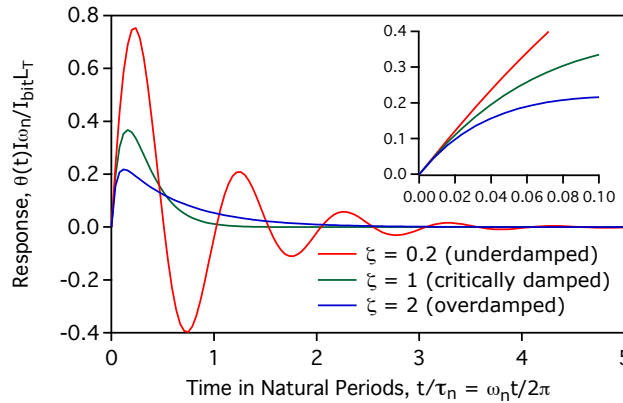

Figure 2. Normalized response of under-, over-, and critically-damped pendulums to an impulse input. The expanded view in the upper right shows that the initial velocity is the same for all three curves.

also be solved for finite pulse lengths[2] and for repeated impulses.[3]

If the force on the thrust stand is time-varying, the response also varies in time and the amplitude depends on the frequency of the applied force compared to the natural frequency of the stand. For a periodic forcing function of the form $F(t) = \overline{F}_t\cos(\omega t)$, the response will initially include a transient component at a frequency of ω_d and a steady state component at the driving frequency ω. After the transient response dies out, the amplitude of the steady state oscillation compared to the deflection $\theta_{st} = \overline{F}_t L/k$ due to a static load of $\overline{F}_t$ is

$$\frac{\overline{\theta}}{\theta_{st}} = \frac{1}{[(1-\Omega^2)^2 + (2\zeta\Omega)^2]^{1/2}}, \quad (13)$$

where $\Omega = \omega/\omega_n$. This function is plotted in Fig. (3) for a range of damping ratios. For critically-damped (and over-damped) pendulums, the response amplitude decays monotonically with input frequency. As expected though, under-damped pendulums can have an amplified response when the driving frequency approaches the resonant frequency of the stand. For frequencies above the resonance, the response is attenuated. The sensitivity of a pendulum thrust stand to dynamic thrust loads therefore varies with frequency.
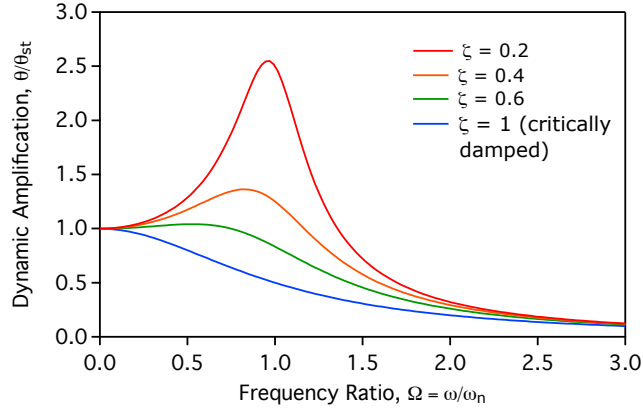
Figure 3. Amplitude of pendulum response due to a periodic force $F(t) = \overline{F}\cos(\omega t)$, normalized by the deflection θ_{st} due to a static load $\overline{F}$.

C.   Thrust Stand Performance Metrics

The quality of thrust measurements depends on seven thrust stand performance metrics, which will be reviewed in this section. Ways to characterize these parameters and achieve high thrust stand performance are discussed in subsequent sections.

1. **Sensitivity.** The thrust stand sensitivity is one of the most important figures of merit, because it largely determines the precision and resolution of thrust measurements. The sensitivity for a steady state thrust measurement can be defined as the deflection achieved for a given applied force in units of [rad/N] . As Eqn. (8) shows, this depends on the length of the moment arm L_t and the effective spring constant k and is therefore a key mechanical design feature of the stand.

   In practice, the sensitivity depends on the ability to measure the deflection, and is often expressed as the voltage output of a position transducer for a given force, [V/N]. There are many ways to measure the angular deflection as a function of time, $\theta(t)$. For small deflections where the small angle approximation is valid, the linear displacement $x(t) \simeq L_{pm}\theta(t)$ at a point a distance L_{pm} from the pivot can be measured. Often, the linear displacement can be measured more accurately than the angular deflection, but at the expense of error introduced by the need to measure L_{pm}. In this case the sensitivity is given by

$$x_{ss}/F_t = L_{pm}L_t/k = L_{pm}L_t/I\omega_n^2 \tag{14}$$

   where x_{ss} is the steady state position. This is typically reported as the position sensor output $V_{ss} = Gx_{ss}$ and G is the sensor responsivity in [V/m]. The responsivity is an important design parameter, and a very sensitive transducer may compensate for small deflections, which may be necessary to remain in the linear regime or because of other constraints.

   For impulse measurements, the sensitivity may be defined as the initial velocity of the pendulum or the maximum deflection obtained for a given impulse, for example

$$\dot{x}(0)/I_{bit} = L_{pm}L_t/I. \tag{15}$$

   This can be similarly translated into the response of a transducer to a given input.

   As noted above, the thrust stand sensitivity can vary with frequency for dynamic thrust loads. To achieve a flat response for relevant thrust input frequencies, the stand should be designed to be under-damped with a damping ratio of $\sim 0.5 - 06$ and a natural frequency much higher than the input frequencies. High natural frequencies can be achieved with high stiffness or low moment of inertia. Of these strategies, decreasing moment of inertia is preferred, otherwise sensitivity (which scales inversely with stiffness) will be sacrificed for flat response. The amplification in response near the resonant frequency has been exploited in at least one design[4] to increase sensitivity. In this approach a pulsed

thruster was fired every half period at the natural frequency of a minimally damped torsional thrust stand in order to amplify the amplitude of the stand oscillation and achieve sub-micronewton sensitivity.

Although the sensitivity can be estimated from the design parameters in Eqn. (14), a value determined by calibration with known forces or impulses should be used to accurately calculate the thrust or impulse bit associated with a measured deflection. Calibration of the thrust stand response is one of the most important steps in thrust measurement, and is discussed in detail in Section III.

2. **Repeatability and Long-term Stability.** The use of a sensitivity calibration performed before and/or after a thrust measurement relies on the assumption that the thrust stand response is repeatable, so this has a first order impact on measurement accuracy. Stability of thrust stand response is also important in long duration, time-resolved thrust measurements. Repeatability can be affected by two factors–drifts which cause a shift in the apparent or real position of the pendulum (zero shifts) and variability in the responsivity G or the effective spring constant k (gain shifts). These effects are often due to temperature changes in mechanical or electronic components or to parasitic spring or friction forces, and must be carefully controlled in the design. Various methods to control or correct for drift and minimize parasitic forces are discussed below. The residual variability in the response must be characterized in repeated calibration measurements under different conditions to determine its contribution to the error estimate, which is discussed in Section V.

3. **Accuracy.** Accuracy is a measure of the error between a thrust stand measurement and the true value of the thrust. In addition to being precise, which is ensured if the thrust stand is sufficiently sensitive, repeatable and not subject to large random errors, it must produce accurate results. High accuracy in a precise thrust measurement is achieved by minimizing systematic errors, and can only be demonstrated by calibration measurements of known forces or impulses. To properly demonstrate that a thrust stand meets a given accuracy requirement, the calibration method must be carefully designed so that it reproduces the conditions of the actual thrust measurement and does not introduce additional systematic errors.

4. **Resolution.** Resolution is defined as the smallest difference between two thrust or impulse inputs that can be reliably distinguished in the thrust stand response. The resolution is ultimately limited by the noise level of the stand's response, so achieving high resolution depends on minimizing noise. Sources of noise typically include the electrical noise associated with sensors, mechanical noise due to vibrations in the environment that are transmitted to the thrust stand, and, on long time scales, variations in thrust stand response that may be caused by periodic changes in temperature, for instance. Thrust stand resolution can be quantified by varying the difference between two input loads until the responses become indistinguishable.[5] In practice this approach may not be feasible, and resolution is often inferred from measured noise levels.

5. **Noise Spectrum.** In some cases, the frequency-dependent thrust noise level generated by the thruster is an important measurement parameter. For instance, the thrusters for the ST7/LISA Pathfinder mission had to demonstrate a thrust noise level $< 0.1\mu\text{N}/\sqrt{\text{Hz}}$ for frequencies between 1 mHz and 4 Hz, a requirement driven by the control algorithm for the disturbance reduction system.[6] In addition to having adequate frequency response, as discussed above, the thrust stand must have a noise floor (noise in the response with no thrust load) significantly lower than the requirement the thruster must meet. The noise floor can be characterized either by amplitude vs frequency or by the power spectral density. This may also be considered the frequency-dependent resolution of the thrust stand.

6. **Response Time.** The thrust stand response time is an important metric for time-resolved measurements, and can be characterized by a number of parameters. Quantitative metrics based on a step input include the rise time (time required to reach 100% of the steady-state value), the peak time (time required to reach the peak response), the maximum overshoot, and the settling time t_s (the time required for the variations around the steady-state value to drop to within 2% of that value). A damping ratio of $0.4 \leq \zeta \leq 0.8$ generally gives good step response. For this range, $t_s = 4/\zeta\omega_n$.

7. **Predictability of the Response.** The response of an ideal pendulum is linear in the small angle approximation presented in Section B. A pendulum thrust stand need not have a linear response, depending on the characteristics of the spring, damper, and position sensor components, but it is good practice to design the stand so this is the case. At a minimum, the transfer function must be known

so that sensitivity calibration data can be interpreted in terms of a physical model. Deviations from the known linear (or nonlinear) functional form measured in a calibration can be used to estimate the contribution of the calibration process to the overall error or to identify systematic problems that need to be resolved before proceeding with a thrust measurement.

Transfer function complexity often depends primarily on the behavior of damping elements in the thrust stand. Active electronic spring/damper systems can be designed to provide a force that is proportional to the deflection or the velocity of the pendulum, or to the integral of the deflection (proportional/integral/derivative or PID control), which results in a much more complex transfer function compared to passive linear elements such as eddy current or viscous dampers. Active control can provide improved transient response, but at the price of greater complexity of the measurement system and analysis.

In addition to these quantitative performance metrics, other considerations such as ease of use and ability to be calibrated effectively play a role in thrust stand design.

D.   Hanging Pendulum Balances

Hanging pendulums are conceptually one of the easiest thrust stands to build and operate, however many designs have evolved into elaborate instruments producing some of the highest fidelity measurements in micropropulsion. In their simplest form, conventional hanging pendulums consist of a vertical arm attached to a top pivot or flexure and a thruster mount or platform at the bottom. They require a displacement sensor, damping mechanism, and calibration system, as do any other free motion thrust stands. Their major advantages lay in their inherent stability and relative ease of use. They have shown to be the least affected by test conditions that cause changes in flexure stiffness, usually due to heating, which results in zero drift problems.

1.   Mechanical Design

Because the effective spring constant in hanging pendulum stands is dominated by the weight term (Eqn. 6), the main design parameter that can influence the sensitivity is the length of the pendulum arm, as apparent in Eqn. 14. Therefore, more sensitive stands typically require large vacuum facilities, and are not well-suited for small test chambers. Another disadvantage also results from the pendulum's motion in the gravitational plane. This not only requires additional attention to the stand's orientation, but also makes that stand's response dependent on the thruster mass. These factors can easily be accounted for and calibrated out as long as they are well understood by the user. Compared with other stand designs, hanging pendulums have several other design challenges. Hanging pendulums are often the least sensitive stand type. However, with proper design and cutting edge materials and equipment, they can achieve incredible accuracies. Both hanging and inverted pendulum types are typically less accurate than torsional based stands, largely due to the lack of counterweights that act to balance the stand, reducing vibration and higher order harmonics.

As with any thrust stand system, its overall ability to reach the required performance goals is largely determined not only by the ingenuity of the particular design, but also by the materials and the supporting hardware used in the build. While simple hanging pendulums are not known for their sensitivity and accuracy compared with their inverted cousins and torsional type stands, several designs have achieved outstanding performance. These stands are usually of a null design, described in more detail in Section G.

An example of a state-of-the-art hanging pendulum thrust stand is the Nanobalance shown schematically in Fig. (4), which was developed for microthruster applications by Thales Alenia Space Italia in co-operation with the Italian National Metrology Institute and Polytechnic of Turin.[5,38] This stand consists of two BeCu plates which hang from flexible BeCu mounts on a rigid block of Zerodur©, a material with a very low coefficient of thermal expansion. The microthruster to be tested is mounted on one of the plates and an identical dummy mass on the other. Both plates are assumed to have the same dynamical behavior, so they respond in the same way to common-mode vibrations from the environment. The displacement of one plate relative to the other is then measured as a thrust response that is free of environmental vibrations. Extensive vibration isolation on the stand and the vacuum facility is also used to minimize disturbance inputs.
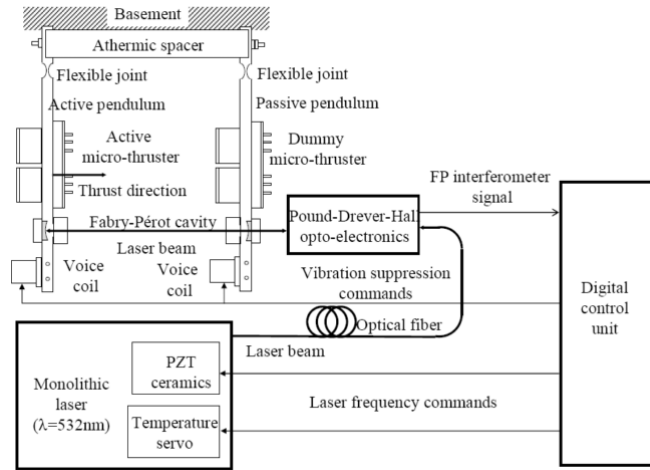
Figure 4. Example of a state-of-the-art hanging pendulum thrust stand.[38]

Two spherical mirrors mounted on the plates form an optical cavity for a Fabry-Perot laser interferometer, allowing very sensitive measurements of the relative displacement. To calibrated electromagnetic actuators (voice coils) that produce a variable force on a permanent magnet by the magnetic field from an electromagnet are used to calibrate each of the pendulums in situ.

Like all pendulum thrust stands, this one is subject to zero drifts caused by changes in the inclination of the mount from which the pendulum plates hang and thermal effects. The Nanobalance incorporates piezoactuators that level the stand based on feedback from an inclinometer mounted on the Zerodur frame. Temperature control and careful choice of materials were used to minimize and correct for thermal drift.

2. Thrust Stand Performance

Using these advanced techniques allows hanging pendulum thrust stands to achieve very high performance. Through sophisticated noise elimination techniques and proper uncertainty analysis, the Nanobalance has demonstrated a force resolution of 0.1 μN and a noise floor spectral density of $< 0.1 \mu N/\sqrt{Hz}$ between 0.1 and 1 Hz (and $< 1 \mu N/\sqrt{Hz}$ down to 1 mHz) over a measurement range of 1 mN.

E. Inverted Pendulum Thrust Stands

An inverted pendulum configuration is often used where a compact, high sensitivity thrust stand is needed. In simplest form, an inverted pendulum consist of a vertical arm attached to a bottom pivot or flexure, and a thruster mounted at the top. With an inverted pendulum configuration, the high stiffness of the elastic spring is countered by the destabilizing influence of the thruster weight, as shown in Eqn. 6. By carefully balancing the length of the pendulum, the thruster mass, and spring stiffness, very large deflections will occur in proportion to applied thrust. Pendulum lengths less than 20 cm are common, permitting several millimeters of deflection inside of vacuum chambers less than 1 m in diameter.[7] Sensitivity is highly dependent on the elastic stiffness of all flexible components of the thrust stand, including electrical and propellant flexures necessary for thruster operation. Due to their compact size, inverted pendulum thrust stands are vulnerable to heat absorbed from the electric thruster. Use of thermal shrouds, and active cooling of critical thrust stand components are often necessary to minimize thermally induced drift of thrust measurements. Most inverted pendulum thrust stands are very sensitive to shifts in the gravity vector. Relatively few designs make use of counterweights to reduce this sensitivity, and those that do have counterweights are not very compact.[8]

1. Mechanical Design

The combination of short pendulum length, and large thrust-induced deflection can result in large angular deflections during tests. Significant rotation of the electric thruster is undesirable where plume diagnostics take place simultaneous with thrust measurement. For this reason, most inverted pendulum thrust stands use parallel linkages to keep the thruster oriented horizontally throughout their range of motion.[7–13] All movement of the thrust stand is mechanically blocked except for straight-line deflection parallel to the thrust vector. There are a number of advantages to non-rotational deflection. The thruster center-of-mass can be positioned anywhere on the thrust stand mounting platform without significant impact on measurement accuracy. Also, magnetic coupling between the electric thruster and the earth's magnetic field should not result in sensitive moments about the pendulum arm. These advantages come at the cost of additional complexity. A parallel linkage thrust stand has roughly four times as many moving parts and joints when compared to a simple inverted pendulum configuration. The additional joints increase the spring stiffness of the thrust stand, requiring additional pendulum height or mass in order to maintain the original sensitivity.

An example of an inverted pendulum thrust stand is shown in Figure (5).[11] Parallel linkages (side plates) are used, which share the vertical load, and maintain the top plate in a horizontal orientation. The thruster is thermally isolated from the thrust stand by a water-cooled mounting post. The entire thrust stand is contained within a temperature-regulated water-cooled enclosure (not shown), except where the cooled mount protrudes. Fine-tuning of thrust stand sensitivity can be accomplished by swapping-out an auxiliary load spring of differing stiffness, using a trial and error process. Robust mechanical stops are provided to limit maximum allowable thrust stand deflection, and prevent accidental collapse. Up to 5 mm of displacement is measured using a linear variable differential transformer (LVDT). The displacement signal is processed by a PID controller, and used to drive two separate electromagnetic actuator coils. Transient and AC signals are sent to the damper coil to provide variable-rate motion damping. The damper signal is carefully balanced to ensure that it contains no DC bias. Slow response DC signals are sent to the water-cooled null coil, which holds the thrust stand at a set-point location. The current flow of the null signal is precisely measured, and is transmitted as the thrust signal. Alternately, the thrust stand can operate in displacement mode, where the LVDT transmits displacement as the thrust signal. A high sensitivity gravitational inclinometer is used to monitor changes in thrust stand inclination due to facility distortions, which are compensated by automatically raising or lowering at the inclination control point. Thrust stands of this size have been used to test 50 kW Hall thrusters, with mass in excess of 100 kg.[9] Similar thrust stands of smaller size have been used to test 0.3 kW Hall thrusters with a mass of 0.9 kg.[7]
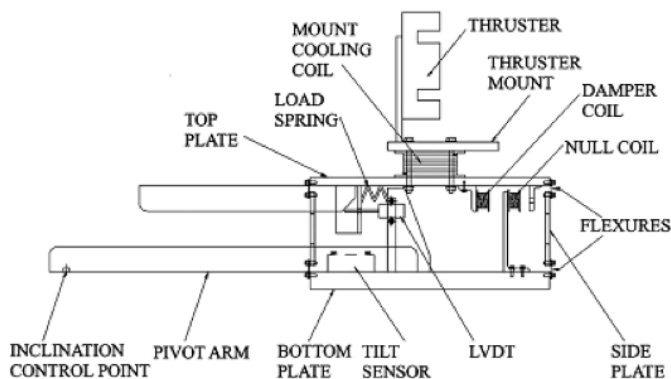

Figure 5. Example of a state-of-the-art inverted pendulum thrust stand.[11]

Many electric propulsion thrusters have thrust-to-weight ratios (T/W) less than 1/500. Consequently, the arm of an inverted pendulum thrust stand is primarily stressed in compression to support the thruster weight. While it is desirable to have highly flexible pivots in the pendulum, they must be stiff enough to safely avoid compressive buckling under the weight of the thruster and resist handling-loads during installation. The pendulum arm should be long enough so that when combined with mounted weight, neutral stability is attainable. The stiffness of electrical conductors, propellant tubing, instrumentation wiring, etc. should be

considered during pendulum arm design. While finely-stranded braided conductors may minimize reaction forces imparted through the thrust stand, internal friction during flexure often results in non-repeatable tares, and unacceptable levels of uncertainty in thrust measurements. Similarly, soft polymer tubing often exhibits viscoelastic behavior, and mechanical properties that vary significantly with temperature. In order to maximize linearity and repeatability, more favorable results are often achieved with solid metallic thrust stand interfaces, operated within their linear elastic range.

2. Thrust Stand Performance

For angles less than 5 degrees, inverted pendulum thrust stand deflection is assumed to be linearly proportional to applied thrust. Measurement error due to nonlinearity is usually much less than other errors introduced by zero drift and vibration. End-to-end calibration, from thrust stand to data recorder, is easily performed by applying known loads to the pendulum, as described in Section III. Another advantage of using parallel linkages in inverted pendulums is that the calibration force can be applied at any point on the rigid platform on which the thruster is mounted. With a single pendulum arm, the calibration forces must either be applied at the same distance from the pivot as the thrust forces, or the location of the calibration forces relative to the thrust forces must be known accurately to scale the resulting torques. Thrust stand sensitivity, noise, and response time are related through the pendulum dynamics reviewed in Section B. One way of expressing sensitivity based on the equations above is as the maximum linear deflection x_{FS} in response to full-scale thrust T, measured at the distance of load application from the pivot L_t, or

$$\frac{x_{FS}}{T} = \frac{L_t^2}{k} \tag{16}$$

Assuming that the moment of inertia is $I \approx L_t^2 M_t$, where M_t is the thruster mass, the natural frequency can be expressed as

$$\omega_n = \sqrt{\frac{k}{L_t^2 M_t}} = \sqrt{\frac{(T/W)g}{x_{FS}}}, \tag{17}$$

where $W = M_t g$ is the weight of the thruster. The thrust-to-weight ratio (T/W) of electric propulsion devices is usually much less than 1. For arcjet thrusters (T/W) is typically 1/200, for Hall thrusters (T/W) is typically 1/300, and for gridded ion thrusters (T/W) is typically 1/600.[7,14]

The characteristic response time for a critically damped thrust stand to settle is approximately one period,

$$\tau_n = 2\pi/\omega_n = 2\pi \sqrt{\frac{x_{FS}}{(T/W)g}}. \tag{18}$$

Full scale deflection is often chosen to be at least two orders of magnitude larger than expected vibrational noise within the vacuum facility. Assuming a noise amplitude of 0.025 mm (1 mil), full scale deflection of 2.5 mm would result in 1% noise. If a Hall thruster were to be tested that had a $(T/W) = 1/300$ the expected settling time would be approximately 1.7 seconds. The actual natural period will be somewhat longer than this, due to the additional mass for the thrust stand top-plate, mounting brackets, tubing and electrical cables. A response time of several seconds is usually adequate for most performance tests, where thermal equilibrium of the thruster may not be reached for many minutes. If necessary, response time can be improved by selecting a smaller full scale deflection x_{FS}, assuming vibration noise levels are acceptable. As mentioned above, the most common cause of thrust measurement error with kW-class thrusters is heat flux, so the thermal design is critical. A properly designed inverted pendulum thrust stand like that shown in Fig.!(5) have demonstrated excellent performance over a range of thrust levels. For example, measurements of a 0.3 kW Hall thruster ranged from 5 mN to 20 mN, with an estimated uncertainty of +/- 1.5%.[7] Thrust measurements of a 1 kW Hall thruster ranged between 80–85 mN, in which calibrations were repeatable to within 1%.[10] Measurement error during calibration up to 400 mN were about +/- 0.6%.[12] Measurements of a 50 kW Hall thruster reached a peak of 2.3 N, with uncertainty estimated to be +/- 2%.[15]

F. Torsional Pendulum Thrust Stands

Unlike both the hanging and inverted pendulum thrust stand configurations, a torsional balance stand's rotational axis is parallel to the gravity vector, making its response independent of thruster mass. This makes it ideal for measuring thrusters that are either changing mass, or facilities that require the ability to test over a very large range of thruster weights. Torsional balances have shown particularly high sensitivity, making them very well-suited for micropropulsion applications. Torsional thrust stands, also called torsion balances, are inherently more stable than inverted pendulum thrust stands[16] and offer a balance of high thrust measurement sensitivity and low environmental noise sensitivity.[17, 18] Due to the size of the beam required for low thrust measurements, torsional thrust stands may pose issues with smaller vacuum chambers. This is especially true for the optimal symmetric arm configuration. While asymmetric configurations are possible (such as a "swinging-gate" configuration), this approach can lead to induced coupling modes with facility vibrations. Torsional thrust stands can resolve thrust measurements from hundreds of nN to a few N,[19–22] which includes a large range of EP devices such as PPTs, FEEP, gridded ion thrusters, and Hall thrusters.

1. Mechanical Design

Figure (6) shows a typical torsional thrust stand design.[23] Torsional thrust stands utilize a long beam attached at two flexural pivots where there exists a torsion spring to provide a restoring force, ideally normal to the gravity vector. An electromagnetic damper provides active damping and an LVDT is used to measure the displacement. Two motors provide active leveling. The effects of gravity have been studied in detail by
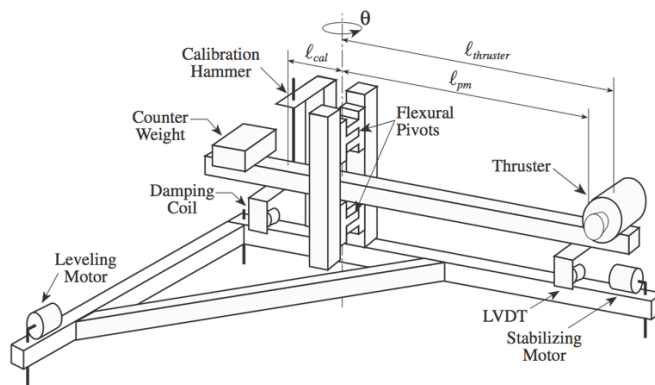

Figure 6. Example of a state-of-the-art torsional pendulum thrust stand.[23]

Ziemer.[23] It affects measurements in two ways: 1) when the vertical rotation axis is offset by some angle, and 2) when the center of mass is not aligned with the vertical rotation axis. In the first case, when the offset angle is positive, the system is stable because the torque works with the spring to resist deflections. As the offset angle grows more negative, the torque will resist the spring constant and, at large enough negative angles, eventually create an unstable system. An analysis shows that three variables can be experimentally changed to reduce this effect: 1) the distance of the center of mass from the rotation axis, 2) the mass of the thruster-counterweight system, and 3) the offset angle. Ziemer notes that it is often the case that the simplest variable to change is the distance of the center of mass from the rotation axis. Counterweights are often used on the side of the beam opposite the thruster in order to place the center of mass of the beam system very near the axis of rotation. This levels the beam and removes the effect of thruster mass from thrust measurements made with the torsional thrust stand.[20, 22–27]

The pivots of the torsional thrust stand can be designed in a number of ways. Some torsional thrust stand variants use thin beryllium[19] or tungsten[20, 26] wire to support the weight of the beam system. These wire diameters are typically on the order of 0.5 mm[26] and the torsion spring constant of the wire provides the restoring force. Other variants use flexural pivots, shown in Figure 1.[21–25] These pivots allow a higher beam system mass (including thruster and counterweights).

Pendulum thrust stands in general are prone to error caused by mechanical connections from propellant lines and power leads, which may not provide stable contributions to the spring force. One solution is to use an inverted cylinder filled with a viscous oil to provide the damping force as well as act as a gas seal so that propellant may flow through the oil and down the long beam to reach the thruster.[24, 28] The amount of viscous damping can be changed by varying the height of the of oil in the cylinder. Another common method for damping uses a passive eddy current damper.[19, 21, 27, 29] This system damps oscillations with eddy currents generated in a conductive plate as it passes through a magnetic field.

Thrust measurements are obtained by determining the angular deflection of the beam. Torsional balances are generally designed so that angular deflections remain within about 5 degrees, where the linear displacement at a specified position along the beam L_{pm} One commonly used method to measure the beam deflection is with a linear variable differential transducer (LVDT), as shown in Figure 1.[2, 16, 23, 24, 28] The LVDT offers high resolution in the small distances over which the beam moves under low thrust levels. Beam deflection can also be measured using a laser triangulation system.[22]

2. Thrust Stand Performance

Torsional thrust stand sensitivity can be changed by a number of factors: torsion spring constant, length of thrust stand beam, and measurement distance from axis of rotation. Typical sensitivities for torsional thrust stands range from 0.046 rad/N in quasi-steady-state mode and 4.51x10-4 rad/μN in dynamic mode.[20] Linearity is proven during all thrust stand calibrations. It has been shown that linearity exists using both piezoelectric hammers[21] and electrostatic fins. Piezoelectric hammers have linearity within 0.99% for a range of 10 mN-s to 750 mN-s, while electrostatic fins were linear to within 0.52% from 0.01 mN-s to 20 mN-s.[27] Repeatability has been measured as 5%[26] for a single-shot PPT while LVDT repeatability is typically less than 0.01%.[21] Overall thrust stand accuracy has been measured as $\pm 1.8 \mu$N[19] for steady-state forces while impulse accuracies are typically 2.1 μN-s for an impulse range of 20-80 μN-s and 0.7 μN-s for an impulse range of 1-10 N-s.[2] Accuracy of the angular displacement has been measured as 2 arcseconds.[26] Typical thrust stand resolutions are less than 1 μN for steady-state forces and less than 1 N-s for impulse measurements.[23] Even smaller resolutions–less than 0.03 μN–have been reported.[25] Yang et al. report resolutions of 0.47 μN-s for impulse bits up to 1,350 μN-s and resolutions of 0.09 μN for steady-state thrust values up to 264 μN.[26]

G.   Steady State Null Balances

The goal of steady state thrust measurement is to determine an unknown force in a laboratory environment, and also track slowly developing variations in that force. A steady state null balance accomplishes this by applying a control force to cancel thrust stand deflection caused by the unknown force. When deflection has been nullified to zero, the control force is assumed to equal the unknown force.

Thrust stands based on spring mass systems must be carefully sized so that the load spring is capable of absorbing the maximum expected magnitude of the unknown force. However, an excessively stiff load spring could result in reduced force measurement resolution. With a null balance, the control force absorbs all of the unknown force, and system spring rate is much less critical. Thrust stands based on spring mass systems are inherently movable, resulting in steady state deflections proportional to thrust. The exact position of thruster surfaces within the test facility is not well controlled, representing a potential source of variability. With a null balance, thruster position is strictly determined by the system set point, except during brief thrust transients.

The mechanical configuration of null balance thrust stands can be very similar to spring-mass type thrust stands. Other than the addition of a force actuator, both stands have many of the same components, including a position sensor. The overall system design of a null balance is much different. While spring-mass thrust balances typically operate open-loop, a null balance uses a tuned feedback loop for stable operation. A PID control system is often employed in order to regulate the control force of the actuator. In order to be usable, the null balance control system must keep the position sensor at the exact set location under steady test conditions. Precise knowledge of the control force is necessary, since this is assumed to equal the

unknown force to be measured. Force actuators are typically electromagnetic, but could be electrostatic. Heat generated within the force actuator may need to be addressed at higher thrust levels.

III. Calibration

Calibration serves three primary purposes. First, the calibration process produces the relationship between deflection or sensor output and thrust or impulse. Second, the accuracy, precision, and repeatability of a thrust stand are determined by repeated application of known forces or impulses, so it is an integral part of the error quantification. Finally, comparison of measured response with the expected theoretical response can reveal systematic problems that would bias the measurements if uncorrected.

A. Application of a Known Force

Laboratory testing of an electric thruster often requires complex interfaces between the thruster and the test facility. Electric current, instrumentation, and various propellants must be provided to the thruster through these interfaces, all of which contribute elastic stiffness and affect the static equilibrium. While these contributions could be characterized individually and summed to calculate the total effective spring constants that determine thrust stand sensitivity,[26] it is much more practical to perform an end-to-end calibration of the entire thrust stand installation, where all elastic and static forces are characterized simultaneously. The calibration process is typically performed with the entire installation fully prepared to test, under vacuum, and only minutes before start-up of the electric thruster. Calibration involves applying known forces F_{cal} at a point L_{cal} from the pivot and monitoring the change in position to determine the thrust stand sensitivity,

$$S_{cal} = \frac{\Delta x_{ss}}{F_{cal}} = \frac{L_{pm}L_{cal}}{I\omega_n^2}. \tag{19}$$

To calculate the steady state thrust of a thruster from a measured displacement Δx_{ss}, this sensitivity must be scaled by the difference in distances from the pivot at which the calibration and thrust forces are applied:

$$F_t = \frac{(L_{cal}/L_t)}{S_{cal}}\Delta x_{ss}. \tag{20}$$

If the calibration forces are applied in the same location as the thrust forces, the ratio $L_{cal}/L_t = 1$ and the thrust force can be determined directly from the calibration curve for a given Δx_{ss} measurement.

Calibration forces can be applied in a number of ways. One common approach is to by loading and unloading weights with known masses on a flexible fiber which is passes over a pulley and attaches to the pendulum. The fiber must be carefully aligned with the thrust vector, and the pulley must be designed with minimum static and dynamic friction so that it transmits all of the force from the weights to the stand. An example of the thrust stand response to this kind of calibration is plotted in Fig. (7). These data were obtained with an inverted pendulum thrust stand similar to that shown in Fig. (5). In this case four calibration weights were hung from a fine chain which passed over a pulley and attached to the rear of the moveable upper platform. The other end of the chain was attached to a cylinder mounted behind the pulley which could be turned with a small DC motor to raise the weights on the cylinder-side of the chain loop, removing the force from the thrust stand. The position of the take-up cylinder was measured with a potentiometer. The change in the LVDT signal, which is proportional to the thrust stand displacement, with application of one, two, three and all four weights was measured. The position of the balance is sensitive to the inclination of the base, so this was actively controlled. The inclination was measured with an inclinometer. The thrust stand base was mounted on a cantilever beam which could be tilted using a DC motor-driven screw to raise or lower one end. The inclinometer output voltage was used as the feedback signal to a software proportional controller which controlled the motor. Application of the weights caused small shifts in the inclination, as shown by the inclinometer signal in Fig. (7), which were then corrected by the controller.

As in this example, the force from the calibration weights is often stepped up and down incrementally using a remotely operated mechanism. The transducer signal after applying weights and the thrust stand zero (transducer output corresponding to no load) after removing the weights, represented by the solid circles
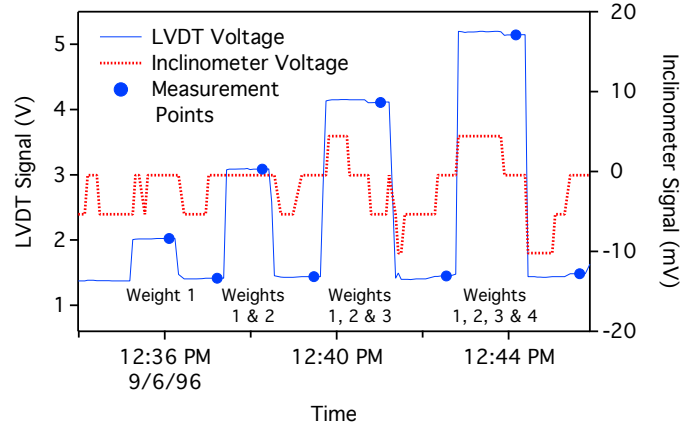
Figure 7. Thrust stand response to application of known forces.

in Fig. (7), are measured to generate a calibration curve. These measurements are often averaged over a number of samples to obtain a good estimate of the mean value, particularly if the transducer signal is noisy. The thrust stand response is defined as the difference between the signal with weights and the zero measured immediately afterwards. This approach automatically corrects for any drift in the thrust stand zero. The calibration process should be designed so that the calibration standards span the range of expected thrust values and are evenly distributed across the range.

Figure (8) shows an example of a calibration curve constructed from $n = 40$ observations of thrust stand response for given input forces similar to those plotted in Fig. (7). The response is modeled as a linear
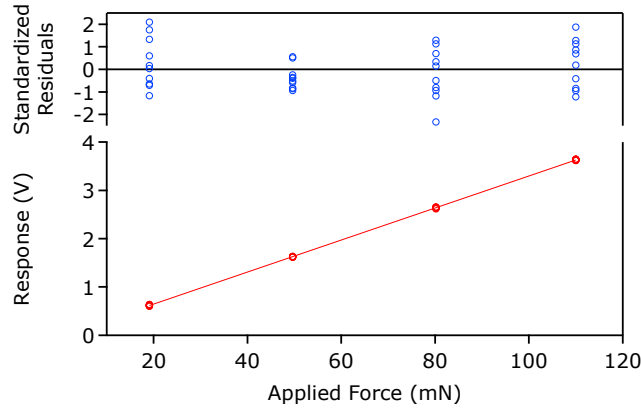

Figure 8. Calibration curve relating thrust stand deflection in terms of LVDT sensor output to applied force.

function of the applied forces,

$$x_i = \beta + \mathcal{S}F_i + u_i, \tag{21}$$

where the x_i are the measured responses to input forces F_i, $\mathcal{S}$ in this case corresponds to the sensitivity of the balance, and the u_i are random disturbances. The intercept β should not be set to zero; it should be estimated from the data. The disturbances are assumed to be normally distributed with a mean of zero and a common variance of σ_x^2. The input forces are assumed to be known without error, so the calibration method must be designed so that the uncertainty of the input loads is much less than that of the stand response. Standard analysis packages can then be used to perform least squares analysis to determine b and S_{cal}, estimates of β and $\mathcal{S}$ which minimize the sum of squared residuals:

$$\sum_{i=1}^{n} u_i^2 = \sum_{i=1}^{n} (x_i - \beta - \mathcal{S}F_i)^2. \tag{22}$$

These regression parameters then yield predicted values of the response for given inputs,

$$\hat{x}_i = b + S_{cal}F_i. \tag{23}$$

The calibration data can be used to calculate an unbiased estimate of the variance σ_x^2 of the random disturbances,

$$\sigma_x^2 \simeq s_x^2 = \frac{\sum_{i=1}^{n}(x_i - b - S_{cal}F_i)^2}{n-2}. \tag{24}$$

The standard deviation s_x is a way to characterize the variability in response with fixed input and plays a key role in the error estimate, discussed in more detail in Section V. The standardized residuals, $e_i/s_x = (\hat{x}_i - x_i)/s_x$ are also plotted in Fig. (8). Residual plots are a very powerful way to evaluate the quality of a fit.[30] In general, if the assumed model is correct, the standardized residuals will fall uniformly between -2 and +2 and will be randomly distributed around zero. A systematic pattern of variation in the residuals can indicate a deviation from linear behavior or other violations of the assumptions on which least squares analysis rely. Another parameter often used in evaluating fits is the square of the correlation coefficient,

$$R^2 = 1 - \frac{\sum(x_i - \hat{x}_i)^2}{\sum(x_i - \bar{x})^2} \tag{25}$$

where $\bar{x}$ is the mean of the measured responses. This is a measure of the proportion of total variability in the x_i that can be explained by the F_{ti}. However, it is only a measure of correlation and a high value does not mean that the data have been well-fit, or that the calibration curve will yield results with low uncertainty. Careful examination of the residuals and a detailed error estimate are recommended for high quality thrust measurements. Lack of linearity or repeatability typically indicates a mechanical problem with the thrust stand installation, such as dragging or unintentional contact as the thrust stand deflects, which should be corrected prior to making thrust measurements.

B.   Application of a Known Impulse

Many thrust stand designs can also be used to make impulsive measurements. However as a general practice it is important to perform a pulsed calibration over the appropriate range to properly characterize these instruments. The most common stands used in impulse measurements are free moving types as they are allowed to oscillate at their natural frequency after a perturbation. These can be hanging or inverted pendulums but are more often torsional balances for improved sensitivity, but usually not nulled type designs. Active electromagnetic dampers may be used to reduce vibrations from the facility, but they are turned off prior to making impulse measurements.[2, 16]

Although thrust stand parameters such as effective spring constant and natural frequency or moment of inertia can be measured to calculate the sensitivity,[16, 26] calibration is usually accomplished by applying known impulses $I_{bit,cal}$ at a point L_{cal} from the pivot and inferring the sensitivity from a change in the dynamic response (such as velocity or peak amplitude or range), similar to the method outlined above for thrust measurements. For example,

$$S_{cal} = \frac{\Delta\dot{x}(0)}{I_{bit,cal}} = \frac{L_{pm}L_{cal}}{I}. \tag{26}$$

As in thrust measurements, this sensitivity must be scaled by the difference in distances from the pivot at which the calibration and thrust forces are applied to calculate the impulse from a measured change in velocity $\Delta\dot{x}(0)$, for instance:

$$I_{bit} = \frac{(L_{cal}/L_t)}{S_{cal}}\Delta\dot{x}(0). \tag{27}$$

Typical calibration methods can be broken down into either contact or non-contact methods. Several contact calibration methods are swinging known masses,[4, 31] impact pendulums,[2] and impact hammers.[23] Non-contact methods include gas dynamic calibration[24] and electrostatic combs.[32] Of these methods the piezoelectric impact hammer and the electrostatic combs are fairly common practice and therefore the two techniques highly recommended for use that will be discussed further in this section.

Electrostatic combs (ESCs) are known for their versatility as they can provide both a steady state force as well as a wide range of impulses. ESCs consists of a set of interlocking non-contacting combs separated by a small gap. One set of the pair is placed on the stand (usually the grounded set) and the other is held and aligned off the stand. The attractive force provided by the combs is a function of the applied voltage, the geometry, and the number of comb pairs in a set.[33] What is important to note is that unlike other capacitively coupled systems, this comb geometry is independent of the gap, or engagement, distance between the combs.[32] This has two major implications for impulse balance calibration. First, it does not require that the location of the stand, and therefore the engagement distance, be known with great accuracy. Second, even though the engagement distance is changing slightly as the stand oscillates, the force applied by the combs does not change throughout the stand's motion.

By accurately controlling the mount of charge, or voltage, on the combs as well as the time that the charge is applied, a well-known impulse can be created. With the proper equipment these calibration devices can operate over a large range of impulse times and magnitudes. ESCs can accurately produce forces from 10s of nN[34] to 10s of mN [27] with errors typically of well less than 1%. To minimize these errors care must be taken to calibrate the combs themselves. This is typically done by placing the combs on a micro-balance scale. Additionally, since the combs are in essence a capacitor, it is important to understand the RLC response of the charging circuit. While this might not be an issue for longer pulse times, voltage overshoot from very short pulses may induce error.[27]

Piezoelectric impactors come in a variety of shapes and sizes, most of which are commercial available and pre-calibrated. The typical application for impulse balance calibration is to strike the stand with the force transducer while recording the output voltage from the transducer. This output voltage is calibrated to correspond to a force, and once integrated as a function of time, yields a total impulse. The force transducer can be mounted on swinging pendulum arm, that when triggered, will strike the stand. Applied impulses in this manner can be varied by adjusting the pendulum release angle and the striking material. Typically the cocked angle and the release trigger are controlled by an electromagnet actuator.[23] Forces ranging from 0.5 N to 100N with errors of 2% can be achieved in this manner.[35] Another mechanism used to swing calibration hammers is a servo motor. These motors can provide very accurate control of position and velocity, improving the accuracy of the applied impulse. Servo-controlled swing arms have been used within the range of 10 mNs to 800 mNs with both a linearity and precision of less than 0.5%.[27]

The known calibration impulse will perturb the natural motion of the stand and cause it to ring or oscillate at its natural frequency. Figure (9) shows a plot of LVDT voltage as a function of time for a torsional balance that has experienced an impulsive perturbation. That impulse has caused the stand to deflect with
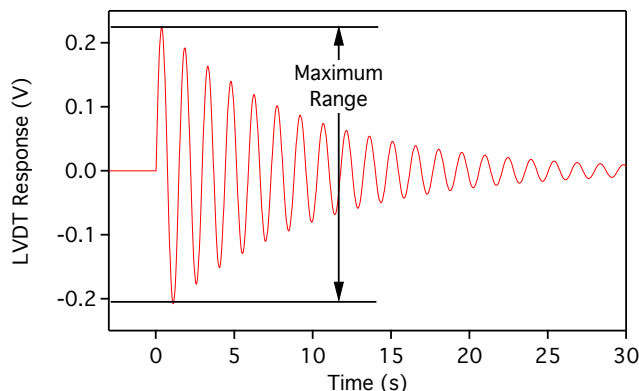

Figure 9. Displacement sensor (LVDT) response as a function of time from an applied impulse.

an initial velocity $\dot{x}(0)$ and a maximum range of travel, defined as the difference between the first peak and the first valley in the oscillatory response. These parameters can be estimated by fitting a damped sinusoid (for underdamped pendulums) to the data. The analysis of linear fits outlined above can be extended to nonlinear fits such as this. In practice, there is often a small amount of background motion or drift that must be subtracted to determine the change in motion due to the impulse. In this case, a damped sinusoid

is also fit to the position history before the impulse and the response is defined as the difference between that and the motion after the impulse.[23] In a careful study of the variance associated with various fitting approaches, Koizumi et al.[2] found that the noise was predominantly at the natural frequency of the stand and could be distinguished from the thruster impulse by fitting the data over a range of $(-2\tau_n, 2\tau_n)$ with a function of the form

$$x(t) = \begin{cases} A_N \sin(\omega_n t) + x(0) \cos(\omega_n t), & t \leq 0 \\ A_F \sin(\omega_n t) + A_N \sin(\omega_n t) + x(0) \cos(\omega_n t) & t > 0, \end{cases} \tag{28}$$

where A_N is the amplitude of the noise and A_F is the amplitude due to the impulse. Their stand was minimally damped, so they did not include a damping term.

If the impulse applied to the stand is known accurately, a good correlation between either the initial velocity or the maximum range and the applied impulse can be determined. An example calibration curve obtained with data similar to that shown in Fig. (9) is plotted in Fig. (10). Figure (11) shows a calibration curve for a torsional balance based on measurements of the initial velocity change due to impact hammer impulses. In
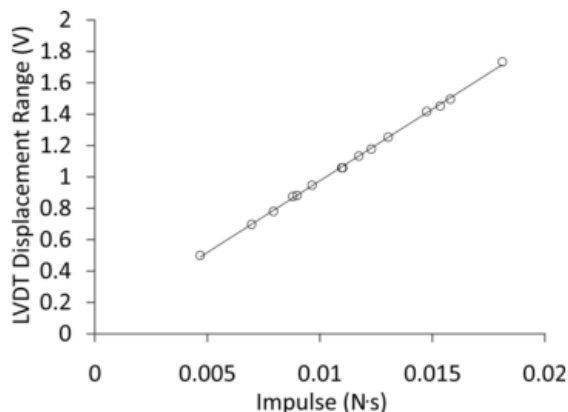

Figure 10. Calibration curve obtained by measuring maximum LVDT signal range (which is proportional to the pendulum amplitude range) as a function of impact hammer impulse values.[21]
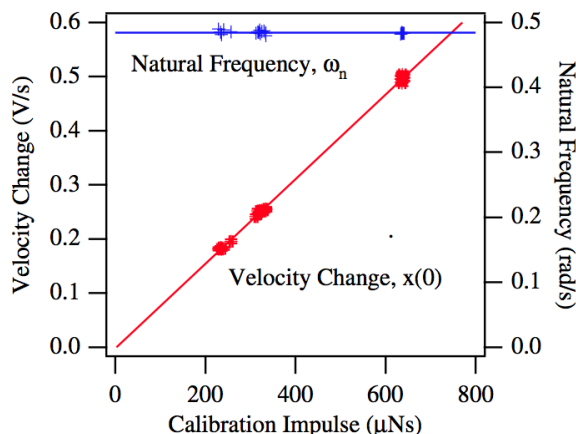

Figure 11. Calibration curve obtained by measuring the initial rate of LVDT signal change (which is proportional to the pendulum velocity in the linear range) as a function of impact hammer impulse values.[21]

both of these examples the transducer signal is not translated into actual displacement or velocity. As long as it is linearly proportional to the motion, the transducer signal can serve as the parameter that is correlated with thrust or impulse. Data such as these can be fit using linear least squares analysis to obtain an estimate of the sensitivity S_{cal}. The same recommendations for the design and analysis of linear calibration curves listed above should be followed with impulsive calibrations as well.

The thruster impulse must approximate a true impulsive load, $F(t) = I_{bit}\delta(t)$. In practice, a linear response can be obtained for finite pulse lengths, as long as they are much shorter than the natural frequency of the stand. Figure (12) shows a range of travel for varying impulse times τ divided by the stand's natural period τ_n. As impulse times become greater than about 1/10 the stand's natural period the results become nonlinear. Therefore it is always recommend that known calibration impulses be applied at much less than the stand's period.
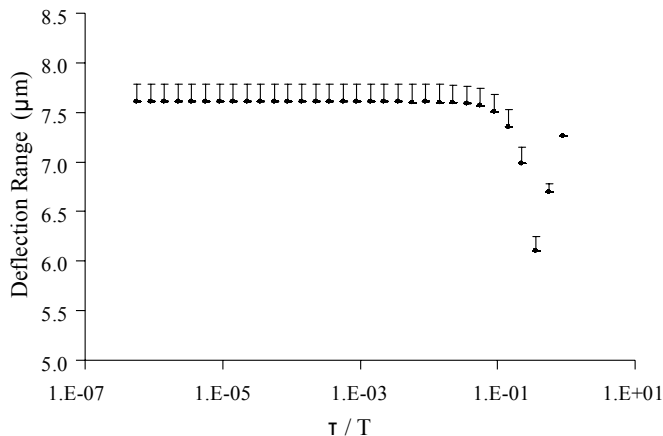

Figure 12. Thrust stand maximum deflection as a function of impulse pulse width normalized by the natural period of the balance.[36]

As with any calibration system it is important to ensure that calibration mechanism itself is well calibrated so that the uncertainty in the applied impulses is very low, a key assumption of the linear least squares analysis. For steady state weight and electrostatic comb calibration systems, the validity of the device is only as good as the scale that was used to measure the weight or force. For piezoelectric hammers, a proper calibration should be performed either by the manufacture, or preferably in-house under the conditions the force transducer will be used. To calibrate a force transducer a free suspended reference mass with an attached accelerometer can be used.[27] Beyond the calibration itself, other factors including strike location and digitization and integration all have to be carefully conducted in order to properly track errors and determine the total accuracy of the impulse calibration system.

IV. Measurement Procedure and Data Reduction

A. Thrust

Data reduction for steady state thrust measurements involves a straightforward application of the calibration curve to calculate thrust. To obtain the most reliable single point measurement of steady state thrust, the following procedure is recommended. Perform a minimum of ten calibrations to generate a calibration curve with small random errors and examine the curve for signs of systematic bias and short term drift, and compare to previous calibrations for signs of long term drift. If the calibration indicates that the thrust stand is performing as expected, start the thruster and allow the operating parameters and thrust stand deflection to stabilize. Obtain a sufficient number of measurements of the thrust stand transducer signal to calculate a mean value with sufficiently small standard error. Turn off the thruster power and flow rate and obtain measurements to characterize the zero (no load) transducer output. The difference between the transducer output with the thruster on and under no load conditions will be considered the response for that operating point. Repeat this measurement cycle if possible to characterize the repeatability of thrust measurements. Perform a minimum of ten calibrations after thruster operation to monitor shifts in the thrust stand sensitivity. If the calibrations taken before and after the thrust measurement indicate that the thrust stand response is stable (i.e. if differences in the calibrations result in contributions to the total error estimate that are tolerable), compute the thrust from the measured response.

An example of the transducer signal obtained with an NSTAR ion thruster[37] following this procedure is plotted in Fig. (13). The sudden drop in LVDT voltage is associated with turning off the high voltage to the engine. The main flow is shut off shortly after that, and small changes in the LVDT signal are apparent as the feed system lines downstream of the valve are evacuated. The zero signal is measured after that point, and then the LVDT signal reflects the start of a calibration sequence. The thrust generated by the mass flow through the engine without power is often significant, and special measures may be required to properly characterize it. Thrust stands are often subject to rapid thermal transients when the engine is first turned off, and the thrust stand zero should be measured before these transients cause significant drift. This may necessitate the use of a flow shutoff valve very near the engine to minimize the blow-down thrust transient.
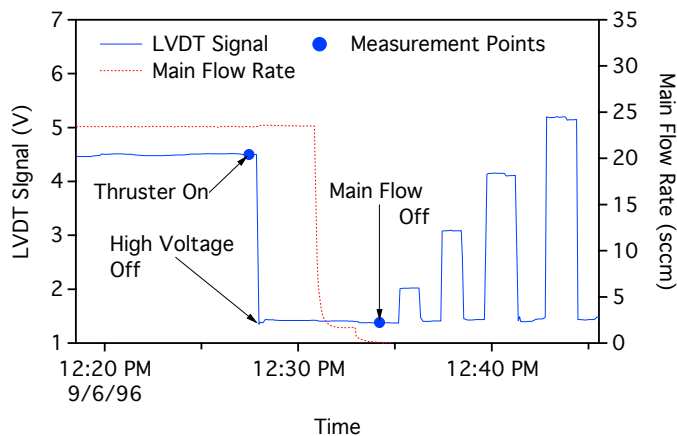

Figure 13. Example of steady state thrust measurement.

Time-resolved thrust measurements may be obtained from the time history of the transducer signal during thruster operation if the thrust stand zero is sufficiently stable. The error can be bounded by measuring the zero before and after thruster operation, and if the time-dependent variation in the zero can be determined, a correction may be applied to the data. Measurements of the temperature of the thrust stand components most susceptible to thermal effects may help guide the correction.[38]

B. Impulse

Data collection for impulse measurements also mirrors the calibration process. After a single impulse, the response data are fitted with a function based on the expected thrust stand dynamics. Figure (14) shows an example of data obtained from a single firing of a pulsed plasma thruster with a torsional pendulum thrust stand. In this case, the data after the pulse have been fitted with a damped sinusoid to estimate the amplitude in the first period. The inset shows a low amplitude oscillation due to environmental vibrations prior to the impulse. This can be fit with a separate damped sinusoid or a range of data before and after the impulse can be fitted with a model that includes noise terms, as discussed above. The fits yield initial velocity or amplitude data that are converted to impulse bit values using the calibration data. Calibration before and after impulse measurements is also recommended to monitor drift in the thrust stand response.

V.   Errors and Uncertainty Analysis

A.   Sources of Error

Instrument errors can be divided into two classes. Random errors are unavoidable at some level and typically are the aggregate result of many small effects, so they tend to follow a normal distribution with a mean of zero. Systematic errors tend to bias the response in a certain direction, so averaging over multiple samples yields a non-zero mean for the error. Different control strategies are employed for random and
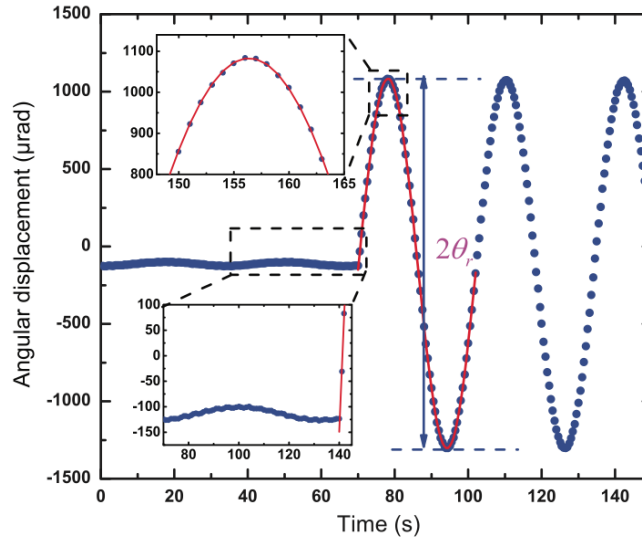
Figure 14. Example of an impulse thrust measurement.[26]

systematic errors. The uncertainty in the mean value due to random errors may be made arbitrarily small in principle by taking more samples of the measured quantity. Unlike random errors, a systematic bias may be characterized experimentally and subtracted from the measurement to produce a corrected result closer to the true value.

Sources of random error in pendulum thrust stand response include natural variability in the mechanical response (stiffness of various elements, for example), electrical noise pickup, which may be much worse during thruster operation, transmission of vibrations from the environment to the thrust stand, vibration due to actuators such as valves on the thrust stand. Additional random errors may enter through the data analysis process, such as errors in the measurement of the distances from the pivot at which thruster and calibration loads are applied. Sources of systematic error include thermal drift, friction between moving and stationary thrust stand components, electromagnetic or electrostatic forces due to high currents or voltages, non-uniform response (amplification or attenuation of higher frequency thrust components, for example) facility effects such as gas currents, dimensional changes in components due to temperature changes, and drift due to changes in the stiffness of cabling or plumbing.

The calibration process also contributes to the total uncertainty. Random variation in the response to known, fixed loads generally represents a major part of the total uncertainty. Calibration in an environment that differs from that during thruster operation can also lead to random errors or bias. For example, the thermal environment, background pressure, gas flow currents, pressure in propellant lines, and current or voltage in electrical lines may be different or absent during calibration. If these are important parameters, they must be reproduced during calibration or characterized separately so that calibration or measurement data can be corrected. Additional sources of error depend on the particular calibration method. For example, the use of weights and a pulley, as described in section III, involves uncertainties in the masses of the weights and the fiber or chain, pulley friction, and potential angular offsets in the fiber from the thrust axis.

B.   Controlling Systematic Errors

The rate of thrust measurement drift due to thermal effects can be minimized with sufficient cooling along the thermal path between the thruster and the stand as well as through the use of materials with high thermal resistance. Placing the stand within an actively cooled shroud enclosure will block plasma impingement and radiative heat transfer to the stand. An effective electrical cable waterfall design can prevent cable expansion and contraction from pushing or pulling on the stand. Additionally, aligning the connection of electrical cables from the base of the stand to the moving assembly orthogonal to the direction of thrust

prevents undesired variable forces on the stand. Active leveling control will eliminate changes in the canting of a thrust stand resulting from thermal fluctuations. Where possible, measuring electrical current in control electronics rather than voltage is advisable in order to avoid errors due to varying voltage drops across cabling caused by temperature fluctuations. Utilizing thermocouples in several locations on the thrust stand can aid in tracking thermal drift effects. As thermal drift is generally unavoidable, frequent stand recalibration is recommended.

Errors caused by friction in the system can be reduced through the use of adequate linear and torsional springs in the thrust stand design. Ensuring that all moving parts are clear of draped electrical cables and other stationary objects through their entire range of motion will minimize intermittent or variable friction and blockage. Attention to cleanliness can prevent unwanted debris from obstructing the motion of the stand. Frequent calibration will also minimize error resulting from gradual changes in friction.

Where applicable, the use of vibrational damping material will minimize measurement error due to external sources of vibration. For null balance thrust stands, a second electromagnetic coil, commonly referred to as a damper coil, can be used to separate vibrational noise from the steady-state thrust signal. Attaching physical stops which restrict the range of motion of the stand will prevent unexpected vibration or impulses from pushing the stand out of range and possibly damaging components.

Where possible, the use of non-ferrous materials in the thrust stand design will mitigate measurement error due to undesired electromagnetic interaction. Maximizing the distance between any magnetic field sources and affected thrust stand components will further reduce measurement errors. Using coaxial or twisted-pair cabling will also reduce interference. If the interaction is unavoidable, characterizing the interaction across the range of possible settings can allow the error to be accounted for during data reduction.[39,40]

C.   Estimating Uncertainties in the Measurement

Despite the best efforts to minimize random errors and eliminate bias, measurement values will always have some uncertainty that represents the range within which the true value is likely to fall. Thrust and impulse measurements should always be reported with an estimate of the uncertainty. The uncertainty analysis involves several steps:

1. **Specify equations used to calculate thrust or impulse.** The equations used in the data analysis should be written explicitly to identify the components subject to error. These are typically like Eqns. 20 and 27 that relate thrust or impulse to a transducer output with certain calibration measurements.

2. **Identify sources of error.** Each part of the calibration, data collection, and data analysis processes should be examined to identify potential sources of systematic or random error. The list in Section A can serve as a guide, but each individual implementation will be subject to unique sources of uncertainty.

3. **Correct for or quantify systematic errors.** The first tactic to employ with systematic bias is to determine the physical cause and attempt to eliminate it. Otherwise the bias should be characterized and a correction applied to the thrust measurement. The uncertainty associated with the correction must be included in the overall uncertainty estimate. If the bias cannot be quantified due to sparse data, the uncorrected measurements should be reported with the probable presence of bias noted, and an uncertainty estimate based on the maximum observed bias included in the overall uncertainty.

4. **Develop an error budget.** The uncertainty associated with each potential error source should be estimated and tabulated to assess the validity of analysis methods and quantify errors in the components of the thrust or impulse calculation. The error budget for a calibration process that employs linear model fits (as illustrated above) is used primarily to verify that the requirements of linear least squares analysis are satisfied. The error budget should verify that the uncertainty in the applied calibration loads is much less than the variability of the thrust stand response. If both the dependent and independent variables have significant uncertainty, conventional least squares analysis should not be used to estimate model parameters. Alternative methods that properly account for uncertainties in both variables are available.[41] Analysis of the linear fits should demonstrate that the linear model is correct and that disturbances are randomly and uniformly distributed.

The uncertainty of each error source should be characterized by either the standard deviation of multiple measurements or a confidence interval based on the standard deviation. The instrument uncertainty for NIST-traceable standards, such as mass balances or force transducers, may also be used to quantify errors. If statistical methods cannot be used to estimate variability in a component, reasonable physical bounds or engineering judgment can be employed, although these methods are discouraged. For components based on model fit parameters, the uncertainty should be based on the estimate of the variance for the dependent variable. For example, the thrust stand sensitivity is determined from the slope of the calibration line and has a standard deviation

$$s_{Scal} = \frac{s_x}{\sqrt{\sum_{i=1}^{n}(F_i - \bar{F})^2}}, \tag{29}$$

where $\bar{F}$ is the average of the forces used in the calibration. The uncertainty in this parameter is reduced by increasing the number of measurements n, ensuring that the calibration measurements spans the range of expected thrust or impulse values, and distributing the calibration points uniformly across the range.

5. **Aggregate component errors to determine thrust error.** The total uncertainty in the thrust measurement depends on the uncertainties of the individual components in the calculation. If the errors are independent, standard error propagation techniques can be used to determine the aggregate effect on calculated thrust or impulse.[42] For example, the uncertainty in thrust F_t calculated using Eqn. 20 is

$$\frac{\sigma_{Ft}}{F_t} = \left[\frac{\sigma_x}{x} + \frac{\sigma_{Scal}}{S_{cal}} + \frac{\sigma_{Lt}}{L_t} + \frac{\sigma_{Lcal}}{L_{cal}} \right]^{1/2}, \tag{30}$$

where σ_x can be approximated by s_x (Eqn. 24), $\sigma_{Scal} \simeq s_{Scal}$, and σ_{Lt} and σ_{Lcal} represent variability in the measurements of L_t and L_{cal}.

In some cases the thrust or impulse can be interpolated directly from a calibration curve. For example, if $L_{cal} = L_t$, the thrust or impulse can be inferred from the plot of response versus calibration loads. The uncertainty in interpolating a value of the independent parameter (F_t for example) from a measurement of the dependent variable (x_t) is given by[43, 44]

$$s_{Ft} = \frac{s_x}{S_{cal}} \left[\frac{1}{N} + \frac{1}{n} + \frac{(\bar{x}_t - \bar{x})^2}{S_{cal}^2 \sum_{i=1}^{n}(F_i - \bar{F})^2} \right]^{1/2}, \tag{31}$$

where n is the number of calibration points, N is the number of repeat measurements performed at that operating condition, $\bar{x}_t$ is the mean of the N repeat measurements of the thrust stand response, $\bar{x}$ is the mean of the n responses to the calibration loads F_i, and $\bar{F}$ is the mean of the n calibration values. This equation accounts for uncertainties in the thrust measurements as well as in the calibration curve. It highlights the value of repeat measurements in reducing uncertainty and the fact that higher sensitivity reduces error.

6. **Control of drift.** Unfortunately, pendulum thrust stands are particularly prone to drift. Periodic calibrations or measurements with check standards can be used to control for changes in precision (susceptibility to random errors) and long term stability (systematic biases).

VI. Conclusions

Pendulum thrust stands can provide very accurate measurements of steady state thrust, time-resolved thrust profiles, and impulse measurements when used properly. Hanging pendulum stands are generally the easiest to implement, but tend to be less sensitive and often require a lot of volume. With highly sensitive displacement measurement techniques and control of environmental vibrations and thermal drift, they can produce high resolution measurements, however. Inverted pendulum stands are typically smaller and more sensitive, and have been employed with great success to measure mN-level thrust in higher power thrusters. Torsional balances appear to be the most appropriate configuration for microthruster measurements (μN-level thrust) and impulse measurements (μNs-level impulse bits). The dimensions of the pendulum, mass of the thruster

and mounting hardware, the stiffness of spring components, damping characteristics of the damping components, and the sensitivity of the displacement transducer are the design parameters that determine the dynamics of the stand and the measurement sensitivity.

Calibration of thrust stands with known forces or impulses is a key part of high fidelity thrust or impulse measurement. A number of force actuators are available that can be very accurately calibrated and used to impart calibration loads to stands. The design of the calibration procedure has a large influence on the uncertainty in the resulting measurement. Calibration and measurement approaches that determine the thrust stand zero (no-load position) and motion (which reflects the influence of environmental noise) for each measurement are the least susceptible to errors caused by drift.

Thrust measurements should always be corrected for known biases and reported with an estimate of the uncertainty based on a statistical analysis of the data. The error estimate involves documentation of the data analysis process, identification and characterization of potential error sources, estimates of the contributions of each error component, and careful aggregation of component errors into an estimate of the uncertainty in the calculated thrust or impulse. Careful design of the thrust balance and calibration procedure and a thorough examination of potential sources of error based on experience reviewed in this paper should result in very accurate, reliable thrust data.

VII.   Acknowledgments

References

[1]Angeles, J., *Dynamic Response of Linear Mechanical Systems: Modeling, Analysis and Simulation*, Springer, New York, NY, 2012.

[2]Koizumi, H., Komurasaki, K., and Arakawa, Y., "Development of thrust stand for low impulse measurement from microthrusters," *Rev. Sci. Inst.*, Vol. 75, No. 10, 2004, pp. 3185–3190.

[3]McFall, K. and Tilley, D., "Low Power Arcjet Performance Evaluation," 24th *International Electric Propulsion Conference*, Moscow, Russia, 1995, IEPC 95-18.

[4]Lake, J., Cavallaro, G., Spanjers, G., Adkison, P., and Dulligan, M., "Resonant operation of a micro-Newton thrust stand," Tech. Rep. AFRL-PR-ED-TP-2002-308, Air Force Research Laboratory, Space and Missile Propulsion Division, Edwards AFB, CA, 2003.

[5]Nicolini, D., Frigot, P., Musso, F., Cesare, S., Castorina, G., Ceruti, L., Bartola, F., Zanella, P., Ceccanti, F., Priami, L., and Paita, L., "Direct Thrust and Thrust Noise Measurements on the LISA Pathfinder Field Emission Thruster IEPC-2009-183," 31st *International Electric Propulsion Conference*, Ann Arbor, MI, 2009, AIAA 2009-183.

[6]Hruby, V. et al., "ST7-DRS Colloid Thruster System Development and Performance Summary," 44th *Joint Propulsion Conference*, Hartford, CT, 2008, AIAA-2008-4824.

[7]Manzella, D. et al., "Evaluation of low power Hall thruster propulsion," 32nd *Joint Propulsion Conference*, Lake Buena Vista, FL, 1996, AIAA 96-2736.

[8]Tartler, B., *Construction and Performance of an Inverted Pendulum Thrust Balance*, Master's thesis, Massachusetts Institute of Technology, Cambridge, MA, 2010.

[9]Manzella, D. and Jankovsky, R., "Laboratory Model 50 kW Hall Thruster," 38th *Joint Propulsion Conference*, Indianapolis, IN, 2002, AIAA 2002-3676.

[10]Garner, C., Brophy, J., Polk, J., and Pless, L., "Cyclic Endurance Test of a SPT-100 Stationary Plasma Thruster," 30th *Joint Propulsion Conference*, Indianapolis, IN, 1994, AIAA 94-2856.

[11]Xu, K. and Walker, M., "High-Power, null-type, inverted pendulum thrust stand," *Rev. Sci. Inst.*, Vol. 80, 2009.

[12]Shabshelowitz, A. and Gallimore, A., "Performance of a Helicon Hall Thruster operating with Xenon, Argon, and Nitrogen," 49th *Joint Propulsion Conference*, Atlanta, GA, 2012, AIAA 2012-4336.

[13]Pote, B. and Hruby, V., "Performance of a Multi-Kilowatt Non-Circular Discharge Hall Thruster," *36th Joint Propulsion Conference*, Huntsville, AL, 2000, AIAA 2000-3249.

[14]Patterson, M. et al., "NASA 30 cm Ion Thruster Development Status," 30th *Joint Propulsion Conference*, Indianapolis, IN, 1994, AIAA 94-2849.

[15]Soulas, G. et al., "Performance Test Results of the NASA-457M v2 Hall Thruster," 49th *Joint Propulsion Conference*, Atlanta, GA, 2012, AIAA 2012-3940.

[16]Haag, T., "Thrust stand for pulsed plasma thrusters," *Rev. Sci. Inst.*, Vol. 68, No. 5, 1997, pp. 2060–2067.

[17]Markusic, T., Jones, J., and Cox, M., "Thrust Stand for Electric Propulsion Performance Evaluation," 40th *Joint Propulsion Conference*, Fort Lauderdale, FL, 2004, AIAA 2004-3441.

[18]Moeller, T. and Polzin, K., "Thrust stand for vertically oriented electric propulsion performance evaluation," 46th *Joint Propulsion Conference*, Nashville, TN, 2010, AIAA 2010-7017.

[19]Zafran, S. and Kemp, R., "Colloid Microthruster Test Stand," *AIAA 3rd Flight Test, Simulation, and Support Conference*, Nashville, TN, 1969, AIAA 1969-314.

[20]Boccaletto, L. and d'Agostino, L., "Design and Testing of a Micro-Newton Thrust Stand for FEEP," 36th *Joint Propulsion Conference*, Huntsville, AL, 2000, AIAA 2000-3268.

[21]Lilly, T., Ketsdever, A., Pancotti, A., and Young, M., "Development of a Specific Impulse Balance for Capillary Discharge Pulsed Plasma Thrusters," *J. Prop. Power*, Vol. 25, No. 3, 2009, pp. 823–826.

[22]Flores, J., Ingle, M., Robinson, N., and Choudhuri, A., "Development of a Torsional Thrust Balance for the performance evaluation of 100mN-5N thrusters," 47th *Joint Propulsion Conference*, San Diego, CA, 2011, AIAA 2011-6016.

[23]Ziemer, J., "Performance Measurements Using a Sub-Micronewton Resolution Thrust Stand," 27th *International Electric Propulsion Conference*, Pasadena, CA, 2001, AIAA 2001-238.

[24]Jamison, A., Ketsdever, A., and Muntz, E., "Gas dynamic calibration of a nano-Newton thrust stand," *Rev. Sci. Inst.*, Vol. 73, No. 10, 2002, pp. 3629–3637.

[25]Gamero-Castao, M. and Hruby, V., "Using a Torsional Balance to Characterize Thrust at Micronewton Levels," 39th *Joint Propulsion Conference*, Huntsville, AL, 2003, AIAA 2003-4537.

[26]Yang, Y., Tu, L., Yang, S., and Luo, J., "A torsion balance for impulse and thrust measurements of micro-Newton thrusters," *Rev. Sci. Inst.*, Vol. 83, No. 3, 2012, 015105.

[27]Pancotti, A., Gilpin, M., and Hilario, M., "Comparison of electrostatic fins with piezoelectric impact hammer techniques to extend impulse calibration range of a torsional thrust stand," *Rev. Sci. Inst.*, Vol. 83, No. 3, 2012, 025109.

[28]Tew, J., Driessche, J. V. D., Lutfy, F., Muntz, E., Wong, J., and Ketsdever, A., "A Thrust Stand Designed for Performance Measurements of the Free Molecule Micro-Resistojet," 36th *Joint Propulsion Conference*, Huntsville, AL, 2000, AIAA 2000-3673.

[29]He, Z., Wu, J., Zhang, D., Lu, G., Liu, Z., and Zhang, R., "Precision electromagnetic calibration technique for micro-Newton thrust stands," *Rev. Sci. Inst.*, Vol. 84, No. 5, 2013, 055107.

[30]Chatterjee, S. and Price, B., *Regression Analysis by Example*, John Wiley and Sons, New York, NY, 1977.

[31]Wilson, M., Bushman, S., and Burton, R., "A Compact Thrust Stand for Pulsed Plasma Thrusters." 25th *International Electric Propulsion Conference*, Cleveland, OH, 1997, IEPC 97-122.

[32]Gamero-Castano, M., Hruby, V., and Martinez-Sanchez, M., "A torsional balance that resolves sub-micro-Newton forces." 27th *International Electric Propulsion Conference*, Pasadena, CA, 2001, AIAA 2001-235.

[33]Johnson, W. and Warne, L., "Electrophysics of micromechanical comb actuators," *J. Microelectromechanical Systems*, Vol. 4, No. 1, 1995, pp. 49–59.

[34]Selden, N. and Ketsdever, A., "Comparison of force balance calibration techniques for the nano-Newton range," *Rev. Sci. Inst.*, Vol. 74, No. 12, 2003, pp. 5249–5254.

[35]Ziemer, J., Cubbin, E., Choueiri, E., and Birx, D., "Performance characterization of a high efficiency gas-fed pulsed plasma thruster," 33rd *Joint Propulsion Conference*, Seattle, WA, 1997, AIAA 2004-2925.

[36]Ketsdever, A., D'Souza, B., and Lee, R., "Thrust Stand Micromass Balance for the Direct Measurement of Specific Impulse," *J. Prop. Power*, Vol. 24, No. 6, 2008, pp. 1376–1381.

[37]Polk, J., Anderson, J., Brophy, J., Rawlin, V., Patterson, M., and Sovey, J., "The Results of an 8200 Hour Wear Test of the NSTAR Ion Thruster," 35th *Joint Propulsion Conference*, Los Angeles, CA, 1999, AIAA-99-2446.

[38]Cesare, S. et al., "Nanobalance: the European balance for micro-propulsion," 31st *International Electric Propulsion Conference*, Ann Arbor, MI, 2009, AIAA 2009-182.

[39]Haag, T., "Thrust stand for high power electric propulsion devices," *Rev. Sci. Inst.*, Vol. 62, No. 5, 1991, pp. 1186–1191.

[40]Kodys, A., Murray, R., Cassady, L., and Choueiri, E., "An Inverted-Pendulum Thrust Stand for High-Power Electric Thrusters," 42nd *Joint Propulsion Conference*, Atlanta, GA, 2006, AIAA 2006-4821.

[41]Fuller, W., *Measurement error models*, John Wiley and Sons, New York, NY, 1987.

[42]Taylor, J., *An Introduction to Error Analysis*, University Science Books, Mill Valley, CA, 1982.

[43]Salter, C., "Error Analysis Using the Variance-Covariance Matrix," *Journal of Chemical Education*, Vol. 77, No. 9, 2000, pp. 1239–1243.

[44]Prichard, L. and Barwick, V., "Preparation of Calibration Curves A Guide to Best Practice," Tech. Rep. LGC/VAM/2003/032, LGC Limited, 2003.